International Journal of Research in Agricultural Sciences
Volume 10, Issue 4, ISSN (Online): 2348 – 3997

Comparative Lipidomic Analysis on Fresh Kernels of Two *Camellia oleifera* Cultivars 'Huaxin' and 'Huashuo' at the Mature Stage

Shunxing Ye
College of Bioscience and Biotechnology, Hunan Agricultural University, 410128, Changsha, China.
Corresponding author email id: yeshunxing2022@163.com

Date of publication (dd/mm/yyyy): 01/09/2023

***Abstract* – *Camellia oleifera* is an evergreen oil-bearing tree that is widely cultivated in China. Camellia oil is considered the healthiest edible oil. However, its lipids distribution has not been well studied and utilized. In the current study, we firstly used the non-targeted LC-MS/MS method to describe the lipid profile of the mature *C. oleifera* kernels. The student's t-test and partial least squares discriminant analysis were used to screen the significant differential lipid (SDLs) between the *C. oleifera* cultivars Huaxin and Huashuo. Through comparative analysis, we identified 121 differential lipids (P- value < 0.05 and VIP > 1.5), and there was a strong correlation between these differential lipids. By using pathway enrichment analysis, we found that the most influential pathway in the two cultivars was the glycerophospholipid metabolism pathway, and that the PLD enzyme may be an important factor to the difference in lipids composition between the two cultivars. Our research provides new ideas for the future development and mining of camellia oil, camellia breeding, and the determination of the maturity and picking periods of Camellia fruit.**

***Keywords* – *Camellia oleifera* Abel, Lipidomics, Non-Targeted LC-MS/MS, PLD Enzyme.**

I. INTRODUCTION

Camellia oleifera Abel. is a small evergreen tree in the Theaceae. It is one of the world's four largest woody oil species (joined with oil palm, olive, and coconut) and it is a widespread oil crop in China, distributed in Jiangxi, Hunan, Fujian, Hainan and Guangxi provinces [1]. *C. oleifera* has important economic value. In 2018, the planting area reached 4,443,300 hectares, and the total output value was about 113.394 billion yuan [2]. In China, the main industry of *C. oleifera* is producing Camellia oil by using its seeds. Camellia oil contains up to 90% of unsaturated fatty acids and over 80% of oleic acid [3]and it is known as the "Oriental Olive Oil" [4]; Camellia oil is rich in a variety of active ingredients, such as squalene, vitamin E, sterols, polyphenols and so on [5]. Besides to as food, Camellia oil is also used as cosmetics, medicine and other industries. Studies have shown that Camellia oil has a good regulatory effect on the human cardiovascular and cerebrovascular, digestion, reproduction, neuroendocrine, and immune systems [6], and long-term consumption of Camellia oil can significantly improve high blood pressure, cardiovascular and cerebrovascular diseases, obesity and other diseases [7].

It is well known that the composition of fatty acids is an important indicator to measure the quality of vegetable oils, and is often used as a parameter to identify a certain kind of oil [8] and the composition, content and ratio of fatty acids determine the nutritional value of edible oils to a large extent [9]. Gas chromatography-mass spectrometry (GC-MS) has been widely used to determine the fatty acid content and fatty acid composition of Camellia oil [10]. Palmitic acid, stearic acid, oleic acid, linoleic acid, arachidonic acid and linolenic acid have been detected already [11]. However, lipids are a group of ubiquitous compounds that perform many key cellular functions, such as membrane biosynthesis, energy storage, and signal molecule production

[12]. In addition to glycerides (GLs), it also includes fatty acyl groups, glycerophospholipids (GPs), sphingolipids (SPs), sterol lipids (STs), glycolipids (SLs), pentenol lipids (PRs) and polyketones (PKs) [13]. To date, other lipid types in *C. oleifera* and the dynamic changes of lipids have not been extensively studied. At present, lipidomics technology based on mass spectrometry technology has been widely used in the research of Chinese herbal medicine and some oil-bearing cash crops. For example, Huang *et al.* used ultra-high performance liquid chromatography-tandem mass spectrometry (UPLC-MS/MS) technology to analyze the lipidomics characteristi--cs and lipid dynamics during the embryonic development of hickory[14]; Chen *et al.* used GC-MS and LC-MS to explain the correspondence between the changes in environment-driven metabolites and lipids and the changes in the biological activity of the black wolfberry fruit[15]; Helen K. Woodfielda *et al.* used lipomics to reveal the details of lipid accumulation during seed development of Brassica napus L[16]. At present, due to the uncertainties in the maturity period and lipid synthesis mechanism of many Camellia cultivars, it is necessary to reveal the lipidomic characteristics of *C. oleifera* kernels and whether it change with cultivars changes. At the same time, the characteristics of the lipid groups of *C. oleifera* will also provide new ideas for future development and mining of Camellia oil, *C. oleifera* breeding and determining the ripening period and picking period of *C. oleifera* fruit [17].

In this study, the non-targeted LC-MS/MS technology was used to analyze the lipidomic characteristics of fresh C. *oleifera* kernels at the mature stage. We also analyzed and compared the lipids composition and relative content of the mature fresh kernels of two large-fruited high-yield *C. oleifera* cultivars 'Huaxin' and 'Huashuo' [18-19]. The analysis includes: (1) the class and relative content of lipids, (2) the screening of significantly different lipids (SDLs), (3) correlation network analysis of the SDLs, and (4) the enrichment of potential differential metabolic pathways. Through comparative analysis, we have deepened our understanding of the lipid components in *C. oleifera* kernels, discussed the lipid synthesis mechanism of the two *C. oleifera* cultivars and the reasons for their differences. Our research can provide guidance for *C. oleifera* breeding, cultivars identification, Camellia oil development and the determination of the maturity picking period of *C. oleifera* fruit.

II. MATERIALS AND METHODS

2.1. *Fresh Kernels of Camellia oleifera Sample Collection*

These mature fruits of *C. oleifera* 'Huaxin' (HX) and 'Huashuo' (HS) were collected from Liuyang County, Hunan Province on 18th October, 2019. Both cultivars were randomly plucked six *C. oleifera* fruits with the similar appearance and growth state from the tree. The kernels of these fresh fruits were randomly divided into three parts (n = 3) and placed in 10 ml EP tube and then frozen with liquid nitrogen immediately. All samples were stored at -80℃ until analyzed.

2.2. *Lipid Extraction*

The procedure for lipid extraction was performed as follows: Firstly, 500μL of lysate which were composed of MeOH: H_2O (1:1, V: V) in to 0.1 g of fresh kernels. The tissues were homogenized at 6500 mhz. The homogeneously mixed sample was incubated overnight at -20℃and then centrifuged for 20 min at 13000 rpm and 4 °C. Then the supernatant was discarded, and 500μL of lysate (DCM: MeOH = 3:1, V: V) as added into the original EP tube. The sample was then vortexed for 60 s and centrifuged for 20 min at 13000 rpm and 4℃. The

supernatant was transferred and freeze-centrifuge to dry; phase buffer B isopropanol (5 mmol/L ammonium formate contained) was added for reconstitution, sonicate for 5 minutes, centrifuge for 20 minutes at 13000 rpm and 4°C. Finally, the supernatants were then transferred to a fresh 2-mL LC/MS glass vial, and enter the LC-MS/MS system for detection and analysis.

2.3. *Chemicals and QC Samples*

The chemicals used were as follows: water (Thermon, USA); acetonitrile (Thermon, USA); methanol (Thermon, USA); isopropanol (Thermon, USA); dichloromethane (Scharlau, Spain); ammonium formate (SIGMA, USA). Six QC samples were mixed from lipid extracts from twenty *C. oleifera* cultivars including HX and HS and used to identify lipids in *C. oleifera* and to ensure the reliability of the results.

2.4. *Lipid Analysis*

LC-MS/MS analyses were performed using a UHPLC system (Exion LCTM Series HPLC, AB Sciex, USA) with a 2.6μ C18 100A column (Phenomen Kinetex ,100 × 2.1 mm) coupled with a Triple - TOF 5600+ (Triple-TOF 5600+; AB Sciex, USA). The mobile phase consisted of A (5 mM HCOONH4 +20% acetonitrile [ACN] + 60% H2O + 20% methanol), and B (10 mM HCOONH4 + isopropanol), and the elution gradient was set as follows: 0 min, 30% B; 1 min, 30% B; 14 min, 95% B; 17 min, 95% B; 17.1min, 30% B; 20 min, 30% B. The injection volumes were 2 μL for both positive- ion and negative-ion modes. In order to obtain MS/MS spectra based on the information during the LC/MS experiment, a triple TOF mass spectrometry was used [20-21]. The mass scanning range of the mass spectrum was 50-1200 Da at collision energy of 40 V, and the scanning time was 20 min. ESI source conditions were as follows: ion source gas 1, 60; ion source gas 2, 60; curtain gas, 35; source temperature, 600 °C or 550°C in positive and negative modes, respectively; ion spray voltage floating, 5500 or -4500 V in positive and negative modes, respectively. Representative LC-MS chromatograms (negative and positive modes) of HX and HS are shown in FigureS1 and S2 in the Supporting Information.

2.5. *Data Processing and Annotation*

The open-source software pipeline MS-DIAL (http://prime.psc.riken.jp/Metabolomics Software/) was wildly used for identification and quantification of small molecules by mass spectral deconvolution [22]. The acquired LC−MS/MS row data were processed by Analysis Base File Converter software (http://www.reifycs.com/Abf Converter/index.html) and converted into ABF format. Then, MS-DIAL can perform peak extraction, alignment, batch effect removal, and metabolite identification based on the converted ABF format. In MS-DIAL, database including LipidBlast was used for metabolites identification [23-24].

2.6. *Statistical Analysis*

The data were UV scaled and processed by SIMCA (Version 14.1, Umetrics, Sweden) for two-dimensional-principal component analysis (2D-PCA). Partial least squares-discriminate analysis (PLS-DA), six-fold cross validation and permutation tests of PLS-DA were processed by the metaX packages of R language [25]. Using only multivariate statistical analysis was easy to cause false positive errors, so we also introduced univariate statistical analysis. Student's t-tests had used to analysze of variance and screen for significantly different lipids (SDLs). The screening criteria were a P-value of less than 0.05 and a Variable Importance in Projection (VIP) value of greater than 1.5, Data processing was carried out by Novogene Co., Ltd. (Beijing, China). In addition,

the correlation network analysis was performed using Cytoscape 3.8.2 (https://cytoscape.org/) [26]. The enrichment Analysis and Pathway Analysis modules of MetaboAnalyst (http://www.metaboanalyst.ca) [27] have helped to qualitatively analyze SDLs and find its metabolic pathways in lipid biosynthesis, other databases including Kyoto Encyclopedia of Genes and Genome (KEGG) pathway database (https://www.kegg.jp/kegg/), human metabolome database (HMDB, http://www.hmdb.ca) and the PubChem database (https://pubchem.ncbi.nlm.nih.gov) were used too. The percentage relative amount of a lipid class was calculated in Microsoft Excel software (Microsoft Corporation, Redmond, WA, USA) by dividing the sum of the peak areas of all lipid metabolites within this lipid class by the sum of the peak areas of all measured lipid metabolites. Heatmaps were drawn using Euclidean distance algorithm and Ward clustering algorithm analytical methods [28].

III. RESULTS

3.1. *Lipidomic Profiling of Camellia oleifera Kernels at Maturity*

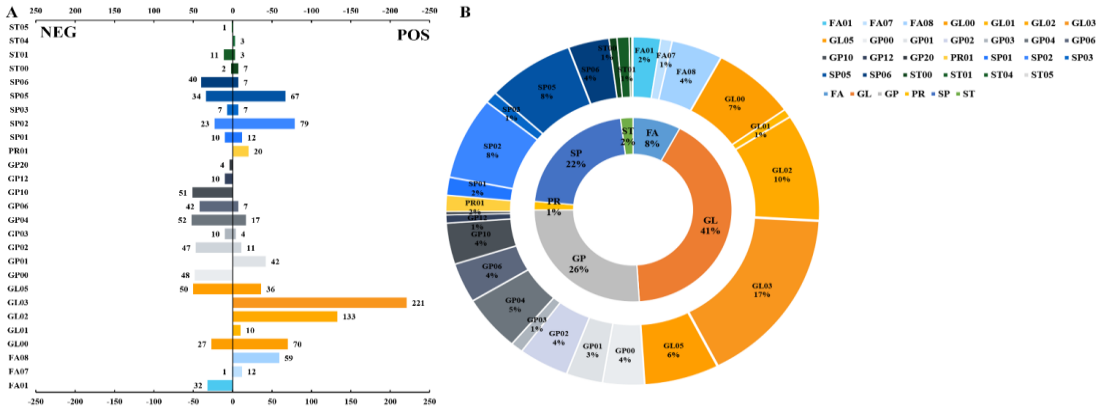

Fig. 1 Identified lipids main class in *Camellia oleifera* kernels at maturity.

(A) Comparison of the identified lipid numbers between positive and negative ion modes.

(B) Percentages of numbers of lipids category (inner circle) and main class (outer circle).

With 6 QC samples were analyzed as a control, 1329 lipid metabolites were identified in the kernels of *C. oleifera* at the mature stage and which we also have involved in previous research [29]. As shown in Fig. 1A, these lipid metabolites can be divided into 6 categories and 27 main class in total, including FAs, GLs, GPs, PRs, SPs, STs categories. Because of the complexity of lipid structure, the polarity of lipids is also different. Some lipids tend to be positively charged, while others tend to be negatively charged, since normally lipidomics using the positive and negative ions detection models [20]. For example, the functional group of Monoradylglyce--rols [GL01], Diradylglycerols [GL02] and Triradylglycerols [GL03] main class including MG, DG, Ether-DG, TG, Ether-TG lipid subclass were carboxyl groups or ester groups [30], So it is easy to be detected in the positive ion mode; SPs are complex lipids that share a common sphingosine skeleton; The C1, C2, and C3 of the sphingosine molecule have functional groups such as hydroxyl, amino, and hydroxyl; Therefore, SPs categories including Sphingoid bases [SP01], Ceramides [SP02], Phosphosphingolipids [SP03], Neutral glycosphingolipids [SP05] and Acidic glycosphingolipids [SP06] subclass were detected in both positive and negative ion modes (Fig. 1A). As shown in Fig. 1B, among the lipid types of fresh kernels of *C. oleifera* at maturity, GLs had the largest number, accounting for 41%, of which diradylglycerols [GL02] and triradylglycerols [GL03] main class had contributed the most, with 10% and 17% respectively. The GPs accounted for 26% ranking second, of

which glycerophospholipids [GP00], glycerophosphoethanolamines [GP02], glycerophosphoglycerols [GP04], glycerophosphoinositols [GP06] and glycerophosphates [GP10] had contributed about 4%-5% respectively; FAs accounted for 8%. STs account for 2% and PRs account for about 2%; The SPs accounted for 22% ranking third, of which ceramides [SP02] and neutral glycosphingolipids [SP05] main class had contributed the most, both with 8%; FAs accounted for 8%, of which FA08 main class had contributed 4%; STs account for 2% and PRs account for about 2%.

3.2. *Comparison of Lipids Composition in HX and HS*

As shown in Figure 3A and 3C, whether in the positive-ion mode or the negative-ion mode, the overall trend of the percentage of the relative concentration of each category of lipids was consistent in these two groups. For example, in the positive-ion mode, GLs accounted for the highest percentage of relative concentration, which was 80.57% in the HX group and 76.39% in the HS group. The percentage of relative concentration of SPs was the second, the percentage of relative concentration of FAs was third (Fig. 2A, 2C); In the negative-mode, the percentage of the relative concentration of GPs was first, which was 72.22% in HX group and 64.99% in HS group relatively. The percentage of the relative concentration of GLs was second, FAs and SPs were ranked third and fourth. It is interesting to note that although there was no big difference in the overall trend of the relative concentration proportions of the lipid categories in these two cultivars, the relative concentration proportions of the main class lipids were very different. Especially obvious in the negative-ion detected mode. As shown in Figure 3D. The percentage of relative concentration of GP10, including PA, LPA subclass lipids, accounted for 44.97% in the HX group, which was nearly one half of the percentage of all detected lipids in negative-ion mode. However, the percentage of the relative concentration in the HS group was only 21.92%, which was only a half of the percentage of the relative concentration in HX group. This disappeared one half of the proportion was displayed in the GP02 main class which consisted by PE, LPE, LNAPE, Ether-PE subclass lipids. The percentage of relative concentration of the GP02 in the HS group accounted for 21.23%, but only 8.15% in the HX group. In addition, there were some commonalities in the composition of the relative concentrations of lipids in these two cultivars. For instance, both in the positive -ion mode and negative -ion mode, the percentage of relative concentration of the FAs categories, FA01, FA07, FA08 main class lipids included, and the SPs categories, SP01, SP02, SP03, SP05, SP06 main class included of the HX cultivar were lower than that of HS cultivar. In positive -ion mode, the percentage of the relative concentration of PRs was also lower than that of HS, accounted for 0.65% and 0.51% respectively (Fig. 2).

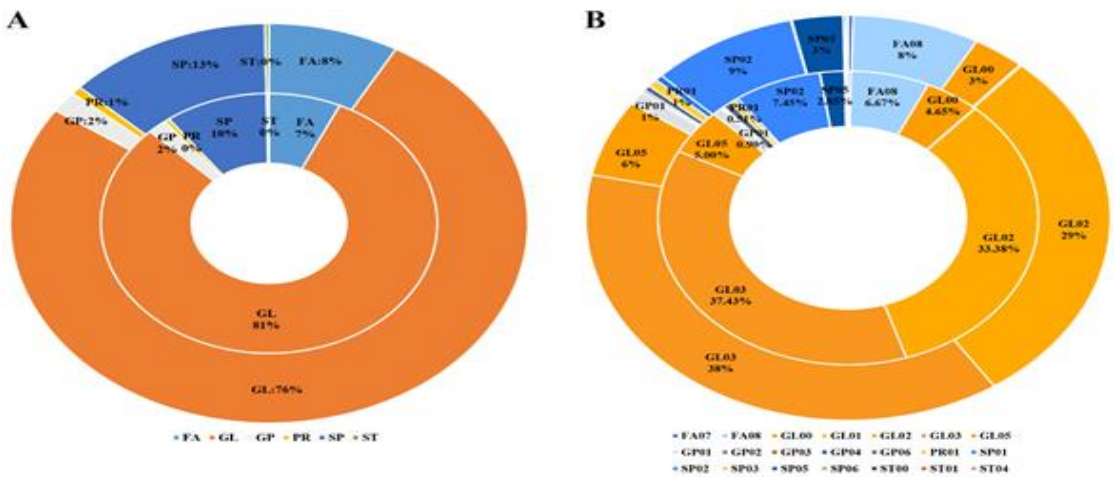

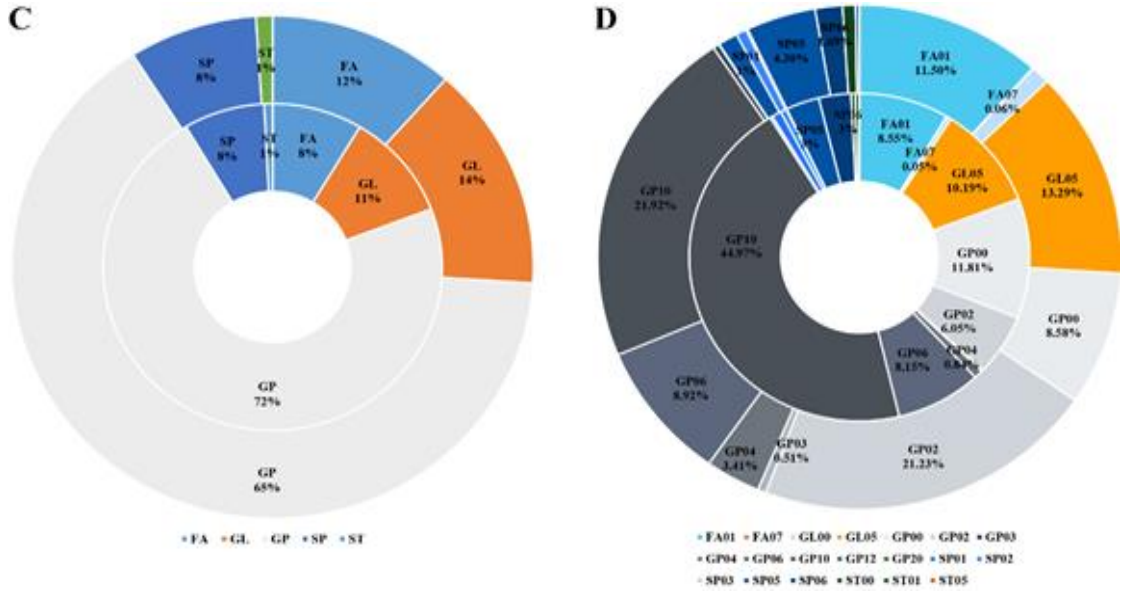

Fig. 2. Comparison of the percentage of the relative concentration of lipids categories and main class subclasses in HX and HS between positive and negative ion modes.

(A) The percentage of the relative concentration of lipids categories in HX (inner circle) and HS (outer circle) in positive-ion mode.

(B) The percentage of the relative concentration of lipids main class in HX (inner circle) and HS (outer circle) in positive-ion mode.

(C) The percentage of the relative concentration of lipids categories in HX (inner circle) and HS (outer circle) in negative-ion mode.

(D) The percentage of the relative concentration of lipids main class in HX (inner circle) and HS (outer circle) in negative-ion mode.

3.3. *Screening of Significantly Different Lipids (SDLs) in HX and HS*

Unsupervised principal component analysis (PCA) was applied to visualize the differences in the lipids pattern among our samples. The results of the PCA analysis are shown in Figure 4A, B. In the positive-mode, the first principal component (PC1) and second principal component (PC2) respectively describe the 45.4% and 20.5% of the variance contained in the data responsible for the grouping of lipid profile of *C. oleifera* Cultivars into two distinct groups; In the negative-mode, the first principal component (PC1) and second principal component (PC2) respectively describe the 48.3% and 16.0% of the variance. No matter in positive or negative mode, HX and HS groups were well separated, which indicated that there was a large variance in the lipid composition of the fresh kernels of HX and HS groups at the mature stage.

Meanwhile supervised PLS-DA and VIP (variable importance in projection) were applied [31-32]. The classification parameters were R2Y = 1.00 in both positive and negative ion mod. Furthermore, Q2 = 0.81 and 0.86 in positive and negative ion mode, respectively, values which were stable and indicated the mode had a good fit and predictive power. Meanwhile, 200 times permutation test was proceeded. The R2 and Q2 intercept values were (0.00, 0.952) and (0.00, -1.82) in positive ion mode, and (0.00, 0.972) and (0.00, -1.85) in negative ion mode (Fig. 3E, 3F). Our results indicate that our PLS-DA model is robust, without over-fitting [33].

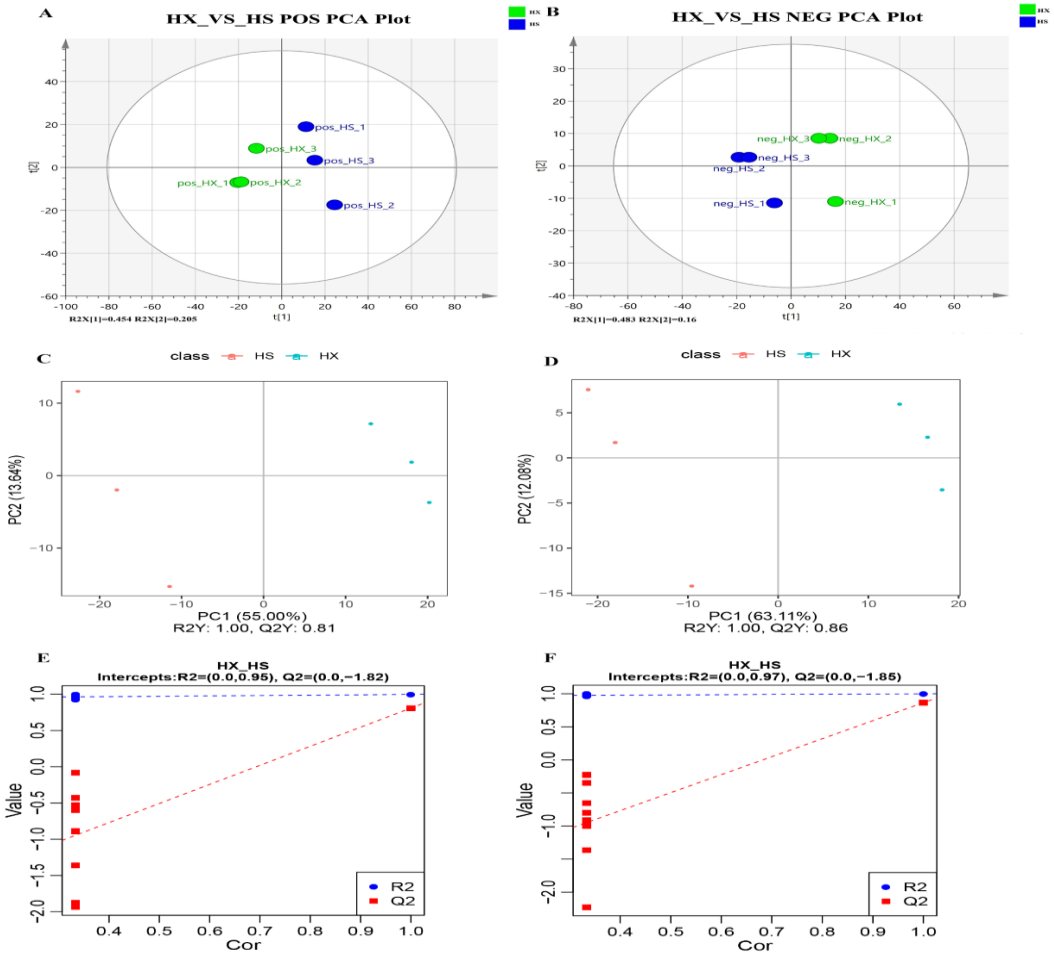

Fig. 3. Principal component analysis and partial least squares discriminant analysis.

(A) PCA-2D score charts based on positive-ion mode, R2X [1] =0.454, R2X [2] =0.205.

(B) PCA-2D score charts in negative-ion mode, R2X [1] =0.483, R2X [2] =0.16.

(C) PLS-DA score charts in positive-ion mode. (D) PLS-DA score charts in negative-ion mode.

(E) PLS-DA permutation plot in positive-ion mode.

(F) PLS-DA permutation plot based on negative-ion mode. R2Y, the interpretability of the model; Q2 Y the predictability of the model.

We extracted VIP values from the variable importance plots of the PLS-DA models. Significantly different lipids (SDLs) were screened based on two criterions: VIP >1.5 and P-value<0.05, According to this criteria, 68 and 53 SDLs were chosen from positive-ion and negative-ion mode, respectively; By comparing HX with HS, 86 SDLs in HX were found to be significantly up-regulated (46 in positive-ion,40 in negative-ion model, respectively), and 35 SDLs were found to be significantly down-regulated (22 in positive-ion,13 in negative-ion model, respectively); HX compared with HS, the most significant difference in the content of SDLs was PA (18:2/18:2) which that HX nearly 900 times higher than HS (HX VS HS, Fold change = 914.22). On the contrary, the content of HBMP (18:1/18:0/18:1) of HX was nearly 100 times lower than that of HS (HX VS HS, Fold change = 0.011). To better understand the chemical differences between HX and HS groups, we drawn the heatmaps of 6 samples in positive-ion and negative-ion modes (Fig. 4A, 4B).

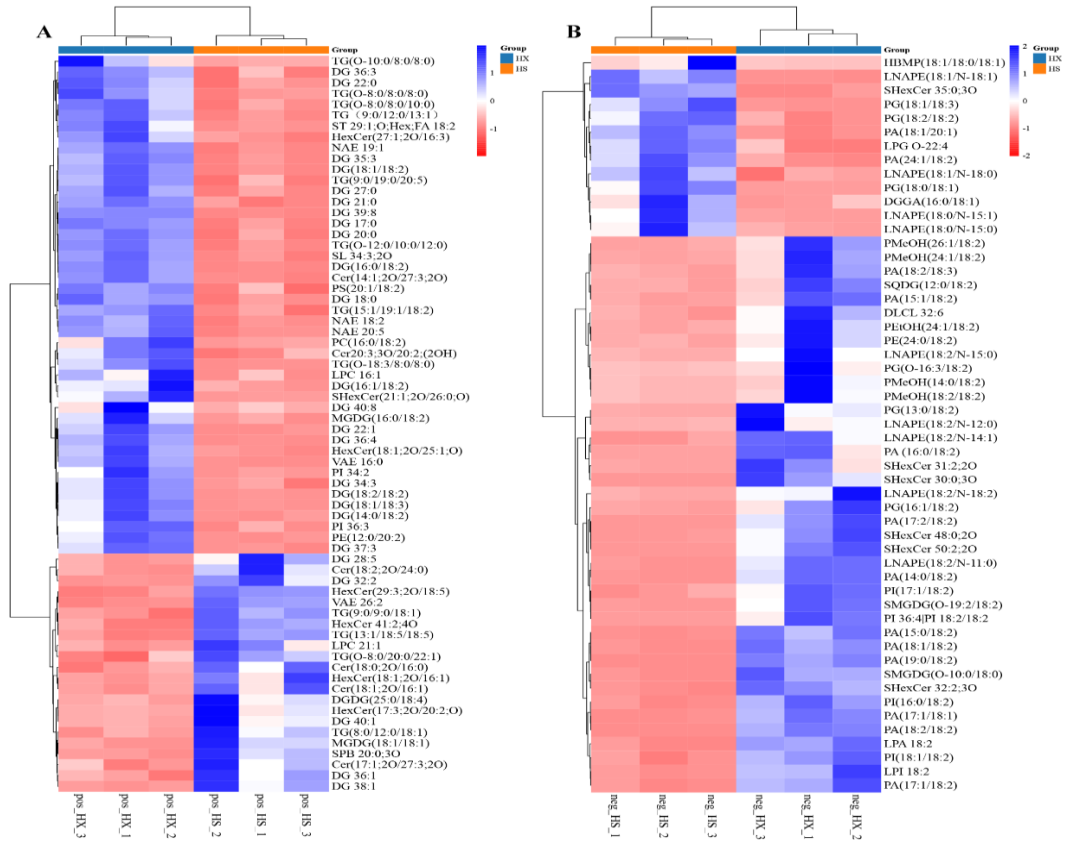

Fig. 4. Heat map analysis of 121 SDLs between HX and HS.

(A) 68 SDLs in positive-ion mode.

(B) 53 SDLs in negative-ion mode.

3.4. *Correlation Network Analysis of the SDLs*

To identify the interactions of the SDLs, a correlation network analysis was performed, and the Pearson correlation analysis had been used to analyze the correlation between SDLs. As shown in Fig. 5, the darker the color of the edge, the stronger the possibility that there was a correlation between these two lipid metabolites, and only P-value lower than 0.05 had been shown. No matter in positive-ion or negative-ion modes, the SDLs were highly correlated, and a change in the concentration of one SDLs may be related to a change in the concentration of other SDLs.

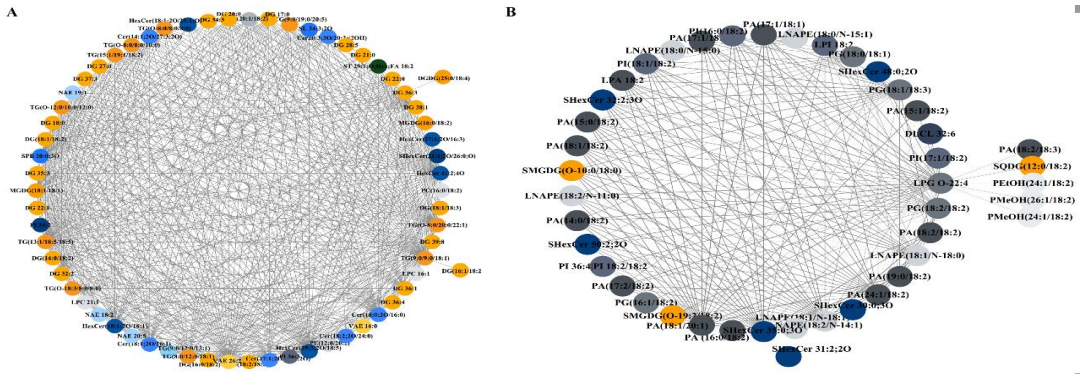

Fig. 5. Pearson correlation network (P-value<0.05) of 121 SDLs in (A) positive-ion mode and (B) negative-ion mode.

Dots of the same color represent the same lipids main class, the width of edges represents the credibility of relevance (P-value), the wider the edge (the smaller the P-value), the higher the credibility of the correlation.

3.5. *Differentially Expressed Lipid Metabolism Pathways between HX and HS*

In order to explore the underlying mechanism that caused changes in the content of lipid metabolites of HX and HS cultivars, we have used MetaboAnalyst tools to enrich the differentially expressed lipid metabolism pathways between HX and HS based on *Arabidopsis thaliana* library. The 121 SDLs were found to be involved in 7 metabolic pathways, the most relevant pathways identified were glycerophospholipid metabolism, glycerolipid metabolism, glycosylphosphatidylinositol (GPI)-anchor biosynthesis, Linoleic acid metabolism, arachidonic acid metabolism, phosphatidylinositol signaling system and alpha-linolenic acid metabolism had little pathway impact (Fig. 6).

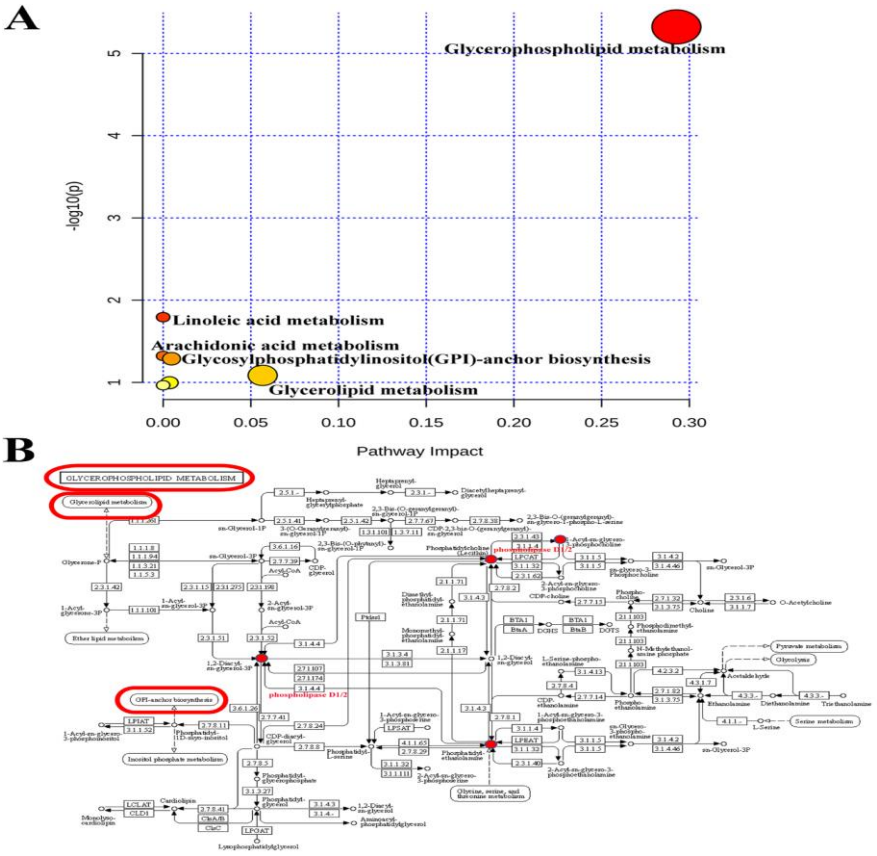

Fig. 6. Analysis of 121 SDLs enrichment pathways and SDLs transition relationship in glycerophospholipid metabolism pathway.

(A) Significant lipid biosynthetic pathways in CL3 and CL53. The X-axis represents the pathway impact, and the Y-axis represents the -ln P-value. The red circles and dots represent major pathways enrichment and high impact values lipids, respectively.

(B) Lipid's transformation relationship in glycerophospholipid metabolism based on KEGG (https://www.kegg.jp/), the red dots represent that the relative concentration of these SDLs in HX is higher than that of HS.

IV. Discussion

Previous studies have found that the fatty acid composition of different *C. oleifera* cultivars will be different [9]. Our research has found that in different *C. oleifera* cultivars the composition of the lipids components is

basically stable in terms of the number of lipid categories and the relative concentration ratio, with GLs and GPs as the main component, SPs and FAs as the second. However, the relative concentration of each lipid main class is different in the HX and HS groups (Fig. 1), indicating that the specific main class lipid composition varies in different cultivars of *C. oleifera*.

In addition, the relative content of GP10 of HS was less than that of HX, but the content of GP02 was more. Therefore, we could speculate that some enzymes or genes in the transformation process of GP02 (PE subclass was the main member) and GP10 (PA subclass was the main member) between HX and HS were very different in the maturation stage of *C. oleifera* kernels. Because phosphatidylethanolamine (PE) is the main source of phosphatidic acid (PA). The discovery of potential differential metabolic pathways through differential lipid enrichment analysis also confirmed our conjecture that phospholipase D enzyme may be a reason for the difference in lipid composition of HX and HS groups' mature kernels (Fig. 6B). Phospholipase D(PLD) is one of the major membrane phospholipid modifying enzymes and which also hydrolyzes glycerophospholipid substrates such as phosphatidylcholine (PC) and phosphatidylethanolamine (PE). Additionally, it cleaves phosphodiester bonds to produce PA and soluble head groups such as choline, ethanolamine, serine, etc. PA can be used as a structural intermediate in eukaryotes membrane lipid synthesis and as a second messenger in many important signal pathways [34-35]. Nowadays PLD has been identified except for tobacco [36], Arabidopsis [37], Oryza sativa [38], Brassica napus [39]. PLD plays a significant role in various cellular processes including programmed cell death, freezing and drought tolerance, mechanical damage, etc. [40]. Furthermore, the key role of PLD in biotechnology has been recognized, oil-TAG synthesis and maintenance of seed quality included [41]. In plants, TAG biosynthesis is carried out through a complex metabolic mechanism, involving a series of different reactions, One of the clearer studies was the Kennedy pathway, and the acylation of the sn-1 and sn-2 positions on glycerol-3-phosphate (G3P) to produce PA. PA phosphatase (PAP) dephosphorylates PA to produce DAG. The sn-3 site of DAG is acylated by DAG acyltransferase (DGAT) to produce TAG. In addition, TAG is produced by phosphatidylcholine diacylglycerol acyltransferase (PDAT) catalyzing the transfer of sn-2 FA from PC to DAG [42-43].

PLD has become an important participant in the regulation of vegetable oil/TAG production. Previous studies have shown that inhibiting the expression of PLD in soybeans will result in highly polyunsaturated PC and lower TAG polyunsaturation in soybean seeds, which indicates that PLD participates in the alternate mechanism of PC conversion to DAG to produce TAG [44]; in Camelina sativa seeds, AtPLD ζ expressing transgenic Camelina plants produced 2–3% higher level of TAG [45]. Our research found that the relative content of GL lipids of HX was higher than that of HS and the content of GPs was higher. In addition, Zhang et al.'s research also found that the oil content and oil body size of Huashuo's seeds picked after the cold dew in mid-October were less than those of Huajin [17]. We speculate that this may be caused by the reduction of PA in HS, which is the precursor of DAG, and the reduction of PA is related to the activity of PLD enzyme. The PLD enzyme activity in HS may be lower than that of HX. This also tells us that in terms of production, the best picking period for HS is not in mid-October after the cold dew. This is consistent with the results of Zhang et al.'s research [17]; If you want to obtain more oil-containing Camellia seeds, HS's picking period should be later than other cultivars; if you want to increase the oil content of HS cultivars, using biotechnology to manually modify its PLD genes may be helpful in the future; Additionally, the differential lipid metabolites we identified can also provide a reference for the development and mining of Camellia oil.

V. CONCLUSION

In our study, lipids in mature kernels of *C. oleifera* were characterized using a non-target LC-MS/MS approach. Totally 121 SDLs were selected from 1329 lipids assigned to 6 categories, 27main class, 71 subclass in HX and HS. In addition, the correlations and related lipids metabolic pathways of these 121 SDLs were analyzed. Seven metabolic pathways associated with changes in lipids were detected. The most significantly pathway of which was glycerophospholipids metabolism, and followed by the glycerolipid metabolism, glycosylphosphatidylinositol (GPI)-anchor biosynthesis metabolism. In addition, combined with the analysis of the relative lipid concentration changes of HX and HS fresh mature kernels, we found that the optimal picking period of HS should be later than HX and that the PLD enzyme activity may be an important factor for the difference of lipids between HX and HS. Our research provides new ideas for the future development and mining of Camellia oil, breeding, and the determination of the maturity and picking periods of fruit.

ACKNOWLEDGMENTS

The authors gratefully acknowledge Liuyang Haoyunwei *Camellia oleifera* Planting Professional Cooperative for the materials collection. This research was funded by 2023 Hunan Agricultural University Undergraduate Innovation and Entrepreneurship Training Program (No. 109).

REFERENCES

[1] Ye Z.C., Wu Y., Muhammad Z., Yan W., Yu J., Zhang J.F., Yao G.L., Hu X.W. Complementary transcriptome and proteome profiling in the mature seeds of Camellia oleifera from Hainan Island. PLoS One, 2020, 15(2): e0226888.
[2] Yu S.H., Zeng Z., Fu W.Y., Xiong X, Liu Y., Tan X.F., Wang ZR, Song J.Q. Analysis of the status quo and countermeasures of the high-quality development of Camellia oleifera industry in Hunan Province. Economic Forest Research, 2019, 37(04): 214-220. (In Chinese).
[3] He S., Ying G. The comprehensive utilization of camellia fruits. American Camellia Yearbook, 1982:104-107.
[4] Xia E.H., Jiang J.J., Huang H., Zhang L.P., Zhang H.B., Gao L.Z. Transcriptome Analysis of the Oil-Rich Tea Plant, Camellia oleifera, Reveals Candidate Genes Related to Lipid Metabolism. PLos One, 2014, 9(8): e104150.
[5] Li C.D., Bei L.W., Jian M.C. Flavonoid triglycosides from the seeds of Camellia oleifera Abel. Chinese Chemical Letters, 2008, 19(11): 1315-1318.
[6] Zhang D.S., Jin Q.Z., Xue Y.L., Zhang D., Wang X.G. Research progress in the nutritional value and adulteration identification of camellia seed oil. China Oils and Fats, 2013, 38(8): 47-50. (In Chinese)
[7] Zhang L.L., Wang Y.M., Wu D.M., Wu D.M., Xu M., Chen J.H. Comparisons of antioxidant activity and total phenolics of Camellia oleifera Abel. fruit hull from different regions of China. Journal of Medicinal Plants Research, 2010, 4(14): 1420-1426.
[8] Lin C.Y., Fan C.L. Fuel properties of biodiesel produced from Camellia oleifera Abel. oil through supercritical-methanol transesterification. Fuel, 2011, 90(6): 2240-2244.
[9] Zeng W, Endo Y. Lipid Characteristics of Camellia Seed Oil. Journal of Oleo Science, 2019, 68(7): 649-658.
[10] Wang Y.P., Fei X.Q., Yao X.H., Wang K.L., Guo S.H., Ren H.D. Principal component analysis and cluster analysis of fatty acids and triglycerides of Camellia oleifera seeds from different origins. China Oils and Fats, 2021, 46(09): 112 -119. (In Chinese)
[11] Chen H., Luo Z.B., Feng X.Y., Zhang D. The fatty acid content, analysis and detection methods and molecular biology research progress of Camellia oleifera oil. Science and Technology of Food Industry, 2019, 40(10): 345-349. (In Chinese)
[12] Rohrig F, Schulze A. The multifaceted roles of fatty acid synthesis in cancer. Nature Reviews Cancer, 2016, 16(11): 732-749.
[13] Fahy E., Subramaniam S., Brown H .A., Glass C.K., Merrill A.H. Jr, Murphy R.C., Raetz C., Russell D.W., Seyama Y., Shaw W., Shimizu T., Spener F., van Meer G., VanNieuwenhze M.S., White S.H., Witztum J.L., Dennis E.A. A comprehensive classification sy--stem for lipids. Journal of Lipid Research, 2005, 46(5): 839–861.
[14] Huang C.Y., Li Y., Wang K.T., Xi J.W., Xu Y.F., Si X.L., Pei D., Lyu S.H., Xia G.H., Wang J.H., Li P P, Ye H.Y., Xing Y.L., Wang Y.G., Huang J.Q. Analysis of lipidomics profile of Carya cathayensis nuts and lipid dynamic changes during embryonic development. Food Chemistry, 2021, 370: 130975.
[15] Chen M.Y., Huang W.J., Yin Z.B., Zhang W.Y., Kong Q., Wu S.W., Li W.Y., Bai Z., Alisdair R. Fernie, Huang X.D., Yan S.J. Environmentally-driven metabolite and lipid variations correspond to altered bioactivities of black wolfberry fruit. Food Chemistry, 2021, 372, 131342.
[16] Woodfield H.K, Cazenave-Gassiot A, Haslam R.P., Guschina I.A., Wenk M.R., Harwood J.L. using lipidomics to reveal details of lipid accumulation in developing seeds from oilseed rape (Brassica napus L.). Biochimica et biophysica acta. Molecular and Cell Biology of Lipids, 2018, 1863(3): 339–348.
[17] Zhang F.H., Li Z., Zhou J.Q., Gu Y.Y., Tan X.F. Comparative study on fruit development and oil synthesis in two cultivars of Camellia oleifera. BMC Plant Biology, 2021. 21(1): 348.
[18] Zhou B.T. Cultivation and management techniques of Hunan Huashuo improved varieties of Camellia oleifera. Southern Agriculture, 2018, 12(15): 42-44. (In Chinese)
[19] Wu L.L., Li J.A., Li Z., Zhang F.H., Tan X.F. Transcriptomic Analyses of Camellia oleifera 'Huaxin' Leaf Reveal Candidate Genes Related to Long-Term Cold Stress. International Journal of Molecular Sciences, 2020, 21(3): 846.
[20] Li M, Li W., Wu J., Zheng Y., Shao J., Li Q., Kang S., Zhang Z., Yue X., Yang M. Quantitative lipidomics reveals alterations in donkey milk lipids according to lactation. Food Chemistry, 2020, 310: 125866.

[21] Li M., Kang S., Zheng Y., Shao J., Zhao H., An Y., Cao G., Li Q., Yue X., Yang M. Comparative metabolomics analysis of donkey colostrum and mature milk using ultra-high-performance liquid tandem chromatography quadrupole time-of-flight mass spectrometry. Journal of Dairy Science, 2020, 103(1): 992-1001.
[22] Tsugawa H, Cajka T, Kind T, Ma Y, Higgins B, Ikeda K, Kanazawa M, VanderGheynst J, Fiehn O, Arita M. MS-DIAL: data-independent MS/MS deconvolution for comprehensive metabolome analysis. Nature Methods, 2015, 12(6): 523-526.
[23] Kind T, Okazaki Y, Saito K, Fiehn O. LipidBlast templates as flexible tools for creating new in-silico tandem mass spectral libraries. Analytical Chemistry, 2014, 86(22): 11024-11027.
[24] Kind T, Tsugawa H, Cajka T, Ma Y, Lai Z, Mehta SS, Wohlgemuth G, Barupal DK, Showalter MR, Arita M, Fiehn O. Identification of small molecules using accurate mass MS/MS search. Mass Spectrometry Reviews, 2018, 37(4): 513-532.
[25] Wen B, Mei Z.L., Zeng C.L., Liu S.Q. metaX: a flexible and comprehensive software for processing metabolomics data. BMC Bioinformatics, 2017, 18(1): 183.
[26] Li M.H., Li Q.L., Kang S.M., Cao X.Y., Zheng Y, Wu J.R., Wu R., Shao J.H., Yang M., Yue X.Q. Characterization and comparison of lipids in bovine colostrum and mature milk based on UHPLC-QTOF-MS lipidomics. Food Research International, 2020, 136: 109490.
[27] Chong J, Xia J Q. Metabo AnalystR: an R package for flexible and reproducible analysis of metabolomics data. Bioinformatics, 2018, 34(24): 4313-4314.
[28] Hewelt-Belka W, Garwolińska D, Młynarczyk M, Kot-Wasik A. Comparative Lipidomic Study of Human Milk from Different Lactation Stages and Milk Formulas. Nutrients, 2020, 12(7): 2165.
[29] Xie H, Chen F, Yin H, Peng G, You C. Characterization and comparison of lipids in Camellia oleifera kernels of XL210 and XL1 based on LC-MS/MS – Science Direct. 2021.
[30] Zhong N.J., Li L., Li B., Lu Q.Y., Liu G.Q. Liquid chromatography analysis of glycerides. Modern Food Science and Technology, 2012, 28(01): 123-126. (In Chinese)
[31] Ashokan M, Ramesha KP, Hallur S, Karthikkeyan G, Rana E, Azharuddin N, Raj S R, Jeyakumar S, Kumaresan A, Kataktalware M A, Das D.N., Keshava Prasad T.S. Differences in milk metabolites in Malnad Gidda (Bos indicus) cows reared under pasture-based feeding system. Scientific Reports, 2021, 11(1): 2831.
[32] Luczaj W, Wroński A, Domingues P, Domingues M R, Skrzydlewska E. Lipidomic Analysis Reveals Specific Differences between Fibroblast and Keratinocyte Ceramide Profile of Patients with Psoriasis Vulgaris. Molecules, 2020, 25(3): 630.
[33] Bian X B, Zhao Y, Xiao S Y, Yang H, Han Y Z, Zhang L X. Metabolome and transcriptome analysis reveals the molecular profiles underlying the ginseng response to rusty root symptoms. BMC Plant Biology, 2021, 21(1): 215.
[34] Pokotylo I, Kravets V, Martinec J, Ruelland E. The phosphatidic acid paradox: Too many actions for one molecule class? Lessons from plants. Progress in Lipid Research, 2018, 71: 43-53.
[35] Kim S.C., Wang X.M. Phosphatidic acid: an emerging versatile class of cellular mediators. Essays in Biochemistry, 2020, 64(3): 533-546.
[36] Lein W, Saalbach G. Cloning and direct G-protein regulation of phospholipase D from tobacco. Biochim Biophys Acta, 2001, 1530(2-3): 172-183.
[37] Eliás M, Potocký M, Cvrcková F, Zarsky V. Molecular diversity of phospholipase D in angiosperms. BMC Genomics, 2002, 3:2.
[38] Li G, Lin F, Xue H W. Genome-wide analysis of the phospholipase D family in Oryza sativa and functional characterization of PLD beta 1 in seed germination. Cell Research, 2007, 17(10): 881-894.
[39] Lu S P, Fadlalla T, Tang S, Li L, Ali U, Li Q, Guo L. Genome-Wide Analysis of Phospholipase D Gene Family and Profiling of Phospholipids under Abiotic Stresses in Brassica napus. Plant And Cell Physiology, 2019, 60(7): 1556-1566.
[40] Wang X M. Regulatory functions of phospholipase D and phosphatidic acid in plant growth, development, and stress responses. Plant Physiology, 2005, 139(2): 566-573.
[41] Deepika D, Singh A. Plant phospholipase D: novel structure, regulatory mechanism, and multifaceted functions with biotechnological application. Critical Reviews in Biotechnology, 2021, 24:1-19.
[42] Bates P D, Browse J. The pathway of triacylglycerol synthesis through phosphatidylcholine in Arabidopsis produces a bottleneck for the accumulation of unusual fatty acids in transgenic seeds. The Plant Journal, 2011, 68(3): 387-399.
[43] Allen D.K., Bates P.D., Tjellström H. Tracking the metabolic pulse of plant lipid production with isotopic labeling and flux analyses: Past, present and future. Progress in Lipid Research, 2015, 58: 97-120.
[44] Lee J, Welti R, Schapaugh W.T., Trick H.N. Phospholipid and triacylglycerol profiles modified by PLD suppression in soybean seed. Plant Biotechnology Journal, 2011, 9(3): 359-372.
[45] Yang W, Wang G, Li J, Bates P D, Wang X, Allen D K. Phospholipase Dζ Enhances Diacylglycerol Flux into Triacylglycerol. Plant Physiology, 2017, 174(1): 110-123.

AUTHOR'S PROFILE

Shunxing Ye, A bachelor student in College of Bioscience and Biotechnology, Hunan Agricultural University. +86-731-84673603, Changsha, China.